Published in final edited form as:
Cell Mol Bioeng. 2009 March 1; 2(1): 57–65. doi:10.1007/s12195-009-0050-1.

Modulation of elasticity in functionally distinct domains of the tropomyosin coiled-coil

Sirish Kaushik Lakkaraju and **Wonmuk Hwang**
Department of Biomedical Engineering, Texas A&M University, College Station TX 77843 Tel.: +1-979-458-0178, Fax: +1-979-845-4450, hwm@tamu.edu

Abstract

Alpha-helical coiled-coils are common protein structural motifs. Whereas vast information is available regarding their structure, folding, and stability, far less is known about their elastic properties, even though they play mechanical roles in many cases such as tropomyosin in muscle contraction or neck stalks of kinesin or myosin motor proteins. Using computer simulations, we characterized elastic properties of coiled-coils, either globally or locally. Global bending stiffness of standard leucine zipper coiled-coils was calculated using normal mode analysis. Mutations in hydrophobic residues involved in the knob-into-hole interface between the two α-helices affect elasticity significantly, whereas charged side chains forming inter-helical salt bridges do not. This suggests that coiled-coils with less regular heptad periodicity may have regional variations in flexibility. We show this by the flexibility map of tropomyosin, which was constructed by a local fluctuation analysis. Overall, flexibility varies by more than twofold and increases towards the C-terminal region of the molecule. Describing the coiled-coil as a twisted tape, it is generally more flexible in the splay bending than in the bending of the broad face. Actin binding sites in α zones show local rigidity minima. Broken core regions due to acidic residues at the hydrophobic face such as the Asp137 and the Glu218 are found to be the most labile with moduli for splay and broad face bending as 70 nm and 116 nm respectively. Such variation in flexibility could be relevant to the tropomyosin function, especially for moving across the non-uniform surface of F-actin to regulate myosin binding.

Keywords

tropomyosin; flexibility map; coiled-coil; persistence length; heptad; biofilament elasticity

1 Introduction

Tropomyosin makes up a large complex family of α-helical coiled coils found in eukaryotes, and is usually seen bound to F-actin.[25] In thin filaments of muscle, it regulates actin-myosin interactions by winding around actin in a right handed fashion and blocking the actin-binding sites of myosin. While precise roles of non-muscle tropomyosin isoforms such as those found in stress fiber assemblies is poorly understood,[19] tropomyosin has been observed to increase actin's persistence length by about 1.5 times.[11] It could thus significantly affect mechanical properties of the cytoskeleton.

Since its 284 pairs of residues (~40 nm) follow mostly an unbroken heptad (seven-residue) periodicity, tropomyosin has been considered as a paradigm of an α-helical coiled-coil.[4] In addition, in muscle isoforms, there is a ~40-residue periodicity where each period is divided into two alternative actin binding α and β zones (Fig. 1). A single tropomyosin molecule can attach to 7 consecutive actin monomers through a strip of negatively charged side chains in either α or β zones. While α zones are more regularly negatively charged,[17] the actual actin

binding residues on the surface of tropomyosin are still not clearly known. Currently accepted "consensus" residues[31] are those initially identified by Phillips.[17;27] Point mutations along the charged surface residues of tropomyosin have been associated with changes in cardiac muscle contractility[9] and dilated cardiomyopathy.[23]

Regulation of myosin binding is achieved by the Ca^{2+} dependent action of tropomyosin and troponin.[4] In the 'off' state, tropomyosin is bound along the outer edge of the F-actin, blocking the myosin binding site. When Ca^{2+} binds to troponin (bound to both tropomyosin and F-actin), it undergoes conformational changes, allowing tropomyosin to move into the groove of F-actin, exposing myosin binding site. Earlier this process was described by a two-state model.[17] More recent observations led to a three-state steric blocking model that consists of the off, blocked, and potentiated states depending on whether tropomyosin covers F-actin's myosin binding site fully, partially, or exposes it.[27] Although details of this process is still unknown, it is likely that tropomyosin undergoes deformation along the non-uniform helical surface of F-actin. Along the molecule there are clusters of alanines which are thought to induce a bend, thereby assisting the coiled-coil to wind around F-actin.[6] However, the energetics of deformation as the molecule binds and moves on F-actin has not been characterized in detail. Mechanical properties of tropomyosin should hence be an important factor for its function.

Previous mechanical characterization of tropomyosin treated it as a homogeneous filament and estimated its global persistence length (l_p) to be about 150 nm.[26] Yet, due to the presence of functionally distinct regions such as for actin binding or for inducing a bend, it is likely that mechanical properties of tropomyosin is nonuniform along the molecule. Here we construct a flexibility map of a cardiac muscle tropomyosin (Protein Data Bank (PDB) ID: 1C1G)[32] using molecular dynamics (MD) simulations. Local coordinate basis named triads were assigned along the length of the molecule and changes in their relative orientation during MD was monitored, from which we calculated local bending and torsional stiffness. For comparison, we also use the standard leucine zipper coiled-coil and study the effect of side chain mutations on its bending stiffness.

While bending stiffness of a single α-helix is not very sensitive to its amino acid sequence,[7;14] we find that coiled-coil has a stronger sequence dependence, contrary to a previous continuum-based theoretical estimate [33] which did not consider energetic contribution by the steric knob-into-hole packing of hydrophobic side chains between two α-helices[8]. Thus coiled-coils with variations in amino acid sequence may not be treated as uniform elastic rods. For tropomyosin, we find that its bending moduli vary by more than twofold, between 220 and 470 nm. Around the broken core region Asn137,[18] it further drops to 116 nm. Hence, analogous to the strength of a chain determined by its weakest link, the 'global' persistence length obtained by considering the entire tropomyosin molecule would be smaller.

The local flexibility map also elucidates how variation in flexibility is tailored for the function of tropomyosin. In particular, α zones are more flexible than β zones, which would be advantageous since tropomyosin binds to the deeper actin groove in the blocked and more in the potentiated states through α zones. Being more flexible, α zones may easily reach their binding site in the actin groove without requiring a rigid-body motion of the entire molecule along F-actin. More generally, local flexibility map of fibrous proteins will provide useful insights into their mechanical function.

2 Theory

2.1 Local Fluctuation Analysis

We first derive the expression for the elastic energy of a continuum rod[10;15] and explain how it is applied to the coiled-coil geometry. Our method is basically the same as the one used by

Choe and Sun for analyzing α-helix elasticity, except that they averaged fluctuation over the length of the molecule.[7]

Let $\mathbf{r}(s)$ be the position vector of the contour of a rod of length L parametrized by the contour length s, such that $\mathbf{r}(0)$ and $\mathbf{r}(L)$ represent two ends of the rod. The unit tangent vector $\mathbf{e}_3(s)$ at a point s is then

$$\mathrm{e}_3 = \frac{dr}{ds}. \tag{1}$$

We introduce two additional unit vectors $\mathbf{e}_1(s)$ and $\mathbf{e}_2(s)$ that are binormal to $\mathbf{e}_3$, so that $\{\mathbf{e}_1, \mathbf{e}_2, \mathbf{e}_3\}$ forms a right-handed *triad*. Choices for $\mathbf{e}_1$ and $\mathbf{e}_2$ are not unique and they only need to be continuously differentiable with respect to s. Typically $\mathbf{e}_1$ and $\mathbf{e}_2$ are chosen based on the cross-sectional geometry of the rod, to better represent the physics.

Now we consider a rod whose equilibrium shape is straight. When it deforms, the curvature vector $\boldsymbol{\omega}$ is related to $\mathbf{e}_3$ by[15]

$$\frac{d\mathrm{e}_3}{ds} = \omega \times \mathrm{e}_3, \tag{2}$$

i.e., $\boldsymbol{\omega}$ is the rate of rotation of the triad along s. When decomposed using triads, ω_1 and ω_2 represent bending of the rod in two directions normal to the contour and ω_3 represents torsion (we ignore stretch in the axial direction, which is usually a good approximation for α-helices and β-sheet filaments since their backbone hydrogen bond network is stiff due to the narrowly distributed hydrogen bond distances[14;24]). If $\mathbf{e}_1$ and $\mathbf{e}_2$ are chosen as principal axes of the cross section of the rod, for a linear elastic material (but not necessarily homogeneous along the length), the elastic energy per unit length at s is given by

$$E(s) = \frac{1}{2}\sum_{i=1}^{3} \kappa_i \omega_i^2. \tag{3}$$

Here, $\kappa_i(s)$ is the stiffness of the rod with respect to the rotation along $\mathbf{e}_i$. The total elastic energy of the rod is then $E_{\mathrm{tot}} = \int_0^L \mathrm{dsE}(s)$. For a rod whose equilibrium shape is not straight, Eq. 3 can be generalized to

$$E(s) = \frac{1}{2}\sum_{i=1}^{3} \kappa_i (\omega_i - \omega_{0i})^2, \tag{4}$$

where $\omega_{0i}(s)$ is the equilibrium curvature of the rod.

If the rod is in thermal equilibrium at temperature T, the average elastic energy stored in the i-th direction for the segment $(s, s + \Delta s)$ satisfies the equipartition theorem[28]

$$\langle E_i(s)\rangle \Delta s = \frac{k_B T}{2} = \frac{1}{2}\kappa_i \langle(\omega_i - \omega_{0i})^2\rangle \Delta s. \tag{5}$$

Here $\langle\cdot\rangle$ denotes ensemble or time average and Δs is chosen small enough so that κ_i, ω_i, and ω_{0i} can be considered invariant over this interval. k_B is Boltzmann constant.

For tropomyosin, we assigned triads as follows. First, centroids for each α-helix were assigned with an interval of 5 residues. These were chosen using the position of ten C_α atoms in an overlapping manner, so that the first centroid is based on residues 1–10, the second on 6–15, *etc*. In total there are 56 centroids on each α-helix. The midpoint between n-th centroids of the two helices then defines the contour vector $\mathbf{r}_n$ ($n = 1 \cdots 56$). We assigned $\mathbf{e}_3 = (\mathbf{r}_{n+1} - \mathbf{r}_n)/|\mathbf{r}_{n+1} - \mathbf{r}_n|$ and $\mathbf{e}_1$ was obtained as a unit vector normal to both $\mathbf{e}_3$ and the vector pointing from centroid n of helix A to that of helix B (choice of helix A and B is arbitrary). This fixes $\mathbf{e}_2 = \mathbf{e}_3 \times \mathbf{e}_1$ (Fig. 1). To construct triad 56 (the last one), a new centroid, 57 was calculated using residues 281–284. But triads 1 and 56 were not used for the actual calculation to eliminate possible end effects. The distance Δs between triads is not uniform across the molecule (*cf.*, Fig. 4a). We used the value of Δs for each successive triad pair averaged over the simulation time.

The curvature vector $\boldsymbol{\omega}_n$ was calculated as follows. Two neighboring triads $\{\mathbf{e}_{ni}\}$ and $\{\mathbf{e}_{(n+1)i}\}$ ($i = 1, 2, 3$) can be related by a transformation matrix $\mathbf{U}$ employing Euler angles

$$\mathrm{e}_{(n+1)i} = \sum_j U_{ij}\mathrm{e}_{nj}. \tag{6}$$

Expressing each unit vector of a triad in terms of three Cartesian components, Eq. 6 can be cast in a matrix form, $\mathbf{E}_{(n+1)} = \mathbf{U}\mathbf{E}_n$. The i-th row of the 3×3 matrix $\mathbf{E}_n$ represents the three cartesian components of $\mathbf{e}_{ni}$. Multiplying $\mathbf{E}^{-1}$ on both sides yields $\mathbf{U}$ and hence the three Euler angles θ_i (the standard notation for Euler angles are α, β, and γ, but we use θ_i for notational simplicity).[2] Components of the curvature vector are then $\omega_{ni} = \theta_i/\Delta s$. In equilibrium, its distribution is Gaussian. By measuring average and variance, Eq. 5 can be used to get κ_i for each triad. Below we present data using the persistence length $l_{pi} = \kappa_i/k_B T$ ($T = 300K$) instead of κ_i. As Fig. 1 shows, l_{p1} is the persistence length with respect to the splay deformation of the molecule as a twisted tape whereas l_{p2} is for bending of the broad face. Torsional rigidity is represented by l_{p3}.

Note that we implicitly assumed that $\mathbf{e}_1$ and $\mathbf{e}_2$ as assigned above are local principal axes. If they are not, there is a term proportional to the product $\omega_1\omega_2$ in Eq. 3. Although it is possible to find principal axes based on the distribution of ω_1 and ω_2, we did not do that since our analysis based on $\mathbf{e}_1$ and $\mathbf{e}_2$ provides an intuitively clear picture of tropomyosin as a twisted tape, while a more accurate set of principal axes may depend on local amino acid sequence, resulting in a less intuitive geometry. Furthermore, as explained below, our simple approach still provides many useful information about the elasticity of tropomyosin.

2.2 Normal Mode Analysis

Determining flexural rigidity $\kappa_b = \min(\kappa_1,\kappa_2)$ and $l_p = \kappa_b/k_B T$ using normal mode analysis (NMA) is well documented in earlier works.[1;14;24] Here we just present the equations used.

For a freely vibrating rod in a linear elastic regime, flexural rigidity can be retrieved from the following relation

$$\kappa_b = \frac{\rho_l \left(\omega^{(m)}\right)^2}{\left(k^{(m)}\right)^4}. \tag{7}$$

Here, ρ_l is the mass per unit length, $\omega(^m)$ is the angular frequency of the m-th bending mode (note that this is different from the component of the curvature vector of the n-th triad ω_{ni} introduced above). $k^{(m)}$ is the wave number given by $\frac{c^{(m)}}{L}$, with $c^{(1)} = 4.7300$, $c^{(2)} = 7.8532$, $c^{(3)} = 10.9956$, *etc.* L is the length of the rod.[24] In principle, κ_b does not depend on the mode number m.[14] In calculations below, we use the first bending mode (m= 1).

3 Results

3.1 Persistence length of a coiled-coil depends on the amino acid sequence

Earlier estimates of the l_p of coiled-coils in experiments were ~150 nm, for the myosin S2 subdomain[13] and tropomyosin As mentioned above, l_p measured from global conformation of the molecule may be affected by flexible points and we expect that a coiled-coil with an ideal heptad periodicity would have a longer l_p.[14] To further study the effect of amino acid composition on stiffness of a coiled-coil, we constructed 112-residue long straight coiled-coils whose heptad sequence was taken from the GCN4 leucine zipper. We introduced point mutations and calculated l_p for each mutant using NMA. Some of these mutants were unstable in MD at 300 K, so local fluctuation analysis could not be applied. As mentioned previously, [14] stiffness and stability represent different parts of the energy landscape: While stiffness relates to the curvature of the conformational energy minimum, stability is a measure of the height of the energy barrier between the conformational minimum and other states. Thus, stiffness can be measured even for weakly stable mutants using NMA.

Table 1 shows that replacing hydrophobic residues with charged ones in *d* positions leads to a progressive decrease in stiffness with an increasing number of mutations. However, point mutations in the hydrophilic outer edge does not affect the stiffness significantly (bottom row in Table 1). Thus while the knob-into-hole packing between hydrophobic faces of α-helices contributes to the stiffness of the coiled-coil, there is no significant contribution by residues on the outer side, including the inter-helical salt bridges formed between charged residues in *e* and *g* positions of the heptad. Instead, these salt bridges are important for maintaining stability of the coiled-coil by protecting the hydrophobic contacts among *a* and *d* residues from water. [16]

In an earlier theoretical study by Wolgemuth and Sun,[33] the adhesion energy between two α-helices was treated as constant under deformation of the coiled-coil. However, our calculation suggests that the steric knob-into-hole packing between hydrophobic side chains in *a* and *d* positions would provide a significant barrier to deformation, rendering l_p of a leucine zipper longer than experimental estimates of coiled-coils that contain regions of varied flexibility or broken heptads.

3.2 Tropomyosin has regions of varied flexibility

Previous crystallographic studies identified regions of varying radius and and pitch across the length of tropomyosin,[32] which suggests that it may not be mechanically uniform along the length. We investigated this by constructing the flexibility map calculated from a 10-ns MD

simulation. Fig. 2 shows example distributions of ω_i. To check whether the simulation time was sufficient, we calculated Δs and the elastic moduli for select triads separately across 2.5 ns intervals during the production run (Fig. 3). Δs does not change notably over time (Fig. 3a). However, measured values of moduli vary more strongly over time. Yet it is not clear whether they fluctuate or drift (Fig. 3b-d). Although a longer MD simulation may reveal a clearer trend, distribution of moduli along the molecule (*i.e.*, as a function of the triad number) is already apparent and is not likely to change in any major way even in longer simulations. Besides, as mentioned briefly in our NMA on leucine zipper, at longer times, parts of the molecule may develop instability, which further complicates elasticity analysis.

The flexibility map reveals several interesting features that could be relevant to the function of tropomyosin. Fig. 4 (a) traces the distance between triads Δs averaged over the production run. It mostly stays within 7.35–7.55 Å, but increases to about 8.3 Å between triads 43–45. This is the region surrounding Glu218. Crystallographic studies show an increased radius in this region due to improper knob into hole packing.[6;18] But Δs stays at the elevated value without any further increase (Fig. 3a). We also did not observe any notable unfolding of this region within the simulation time.

Comparing bending stiffness in two directions, if the molecule is depicted as a twisted tape, it is more flexible with respect to splay (l_{p1}) than to bending (l_{p2}) (Fig. 4b,c). The regions at Asp137 (*d* position) and Glu218 (*a* position) are highly flexible ($l_{p1} \sim$ 250 nm, 116 nm, and $l_{p2} \sim$ 68 nm, 196 nm respectively). As we see from Table. 1, non-hydrophobic residues in the *a* & *d* positions reduce the stiffness of the coiled-coil. Improper knob into hole packing and increased spacing between the two α-helices as explained above, could be destabilizing the molecule at these regions, leading to increased flexibility.

Fig. 4(b) also reveals that along all the α-zones (orange filled circles), the putative actin binding sites (magenta stars) form local rigidity minima, which would assist with actin binding. These sites are composed of regular repeats of negatively charged residues in *b* and *f* positions of the heptad.[4] The enhanced flexibility is likely because of more polar residues occupying the *a* and *d* positions at the hydrophobic core (such as Tyr or Gln in the *d* position), which is consistent with our mutational analysis of leucine zipper (Table 1). In the blocked state and further in the potentiated state, when the molecule moves into the actin groove, flexible actin binding interfaces would render the transition as a succession of local movements, so that the actin binding domains first reach the binding site, followed by the movement of the rest in a deformable way. Otherwise, the entire 40-nm long molecule would have to move on actin more as a rigid body, which would be a difficult task. Likewise, flexible domains would assist with reverse transitions out of the actin groove.

Overall, flexibilities in all three directions of deformation increase towards the C-terminus, including torsional rigidity, l_{p3} (Fig. 4). The globular head of the troponin complex binds to the region around triad 38, and the tail of troponin T binds to the C-terminal part of tropomyosin. The C-terminal half of tropomyosin interacts with the troponin complex, while the N-terminal half may need to move in a more isolated fashion, which may be why the N-terminal part is stiffer. Furthermore, we did not find any particular reduction in flexibility in regions of alanine clusters. Thus, although they may induce a bend through improper knob-into-hole packing,[4] they are not necessarily more flexible.

In this long coiled-coil, backbone hydrogen bonds in each α-helix do not stay always formed throughout the simulation. Since earlier studies indicated its importance in elasticity of α-helices[14] and β-sheets,[24] we plotted percentage of time that they are formed within five residues for each triad (Fig. 5). Hydrogen bonds mostly stay intact with occupancy higher than 80%. Regions where the hydrogen bond occupancy is low correspond to flexible regions shown in

Fig. 4, such as triads 27 and 43. In these regions, deformation is accompanied by breakage of backbone hydrogen bonds, thus their elastic properties are likely nonlinear. Local persistence length, or stiffness κ_i (Eg. 3) are thus simple indicators of local lability, but these regions should not be regarded as linearly elastic.

4 Discussion

To a first approximation, a fibrous protein may be described as a uniform elastic rod. This is the case for filaments such as F-actin and microtubule, which are built by assembly of identical subunits. Earlier works suggested that elasticity of α-helices is roughly independent of the amino acid sequence, so they can be described as mechanically uniform.[7;14] Coiled-coils, however, have stronger sequence dependence in its elasticity. We found that mutations in the *a* and *d* positions of the leucine-zipper coiled-coil affects its elasticity whereas those on other positions do not. Residues on *a* and *d* positions are typically hydrophobic and make knob-into-hole packing to hold the two α-helices together. Charged side chains on *e* and *g* positions form salt bridges, which, although important for stability,[34] we find do not affect the elasticity significantly. Here we emphasize the difference between stability and flexibility: flexibility is determined by the local curvature of the conformational free energy minimum of the molecule, while stability is related to the height of the energy barrier to escape from this minimum. In mechanical terms, stability can be related to the yield strength. Also, as our hydrogen bond analysis in Fig. 5 shows, regions of high flexibility may not follow linear elasticity, so that their elastic moduli should be interpreted with caution.

Our analysis thus shows that long coiled-coils may not be treated as uniform elastic rods. Global persistence length or flexural rigidity would only be a coarse indicator. In the past, the coiled-coil neck of Rad50 has been observed to have regions of varying flexibility.[21] Common variations in the heptad periodicity such as stutters (deletion of 3 residues in a heptad) and stammers (deletion of 4 residues) have also been suggested to lead to local flexibility changes.[5]

We find that tropomyosin, despite having a sequence that mostly follows the heptad periodicity, also has varied rigidities between functionally distinct domains across its length (Fig. 4). Overall the molecule is more flexible in the C-terminal region, and in the actin binding sites. Regions with charged residues at the hydrophobic face (Asp137 and Glu218) are particularly flexible. Such regular variations in flexibility by more than twofold may have implications in tropomyosin function, in particular for its movement along the actin filament. More structural data regarding tropomyosin bound to F-actin, and/or with other tropomyosin binding proteins such as the troponin complex, would further allow to elucidate how the distribution of elastic properties control the tropomyosin function.

5 Simulation Details

We used CHARMM[3] version c34b1 for simulations and Visual Molecular Dynamics (VMD) [12] for visualizations. The param19 force field in CHARMM was used.[20] For NMA of leucine zipper structures, straight coiled-coils were constructed using a C-code provided by Offer.[22] They were energy minimized in a two-step process. First, backbone atoms were constrained harmonically with a spring constant of 5 kcal/(mol·Å^2) and side-chains were energy minimized using the adopted basis Newton-Raphson (ABNR) method until the energy change between successive minimization steps reached less than the default tolerance of CHARMM. Next, constraints were removed and the entire molecule was again fully energy minimized. The VIBRA facility of CHARMM was used to calculate normal modes and their frequencies. Stiffness was calculated using Eq. 7.

For the flexibility map, simulations were carried out on the 1C1G structure. Although its 7-Å resolution is not high, since coiled-coil has a well-defined geometry due to intrahelical backbone hydrogen bonds and knob-into-hole packing between helices,[8] uncertainty would be more in the global conformation of the 40-Å long molecule and exposed side chains, which anyway fluctuate during MD simulations.

To incorporate the effect of solvation effects, we used the ACE2 continuum solvent model in CHARMM.[29;30] It has been previously shown that water molecules do not affect the elasticity of α-helices much, although stability may be affected more.[7;14] This is because the elasticity is determined mainly by the network of backbone hydrogen bonds rather than by interaction among side chains and water molecules. It is expected that the same is true for coiled-coils, which, in addition to backbone hydrogen bonds, have the knob-into-hole packing of hydrophobic residues as a major determinant of elasticity.

After energy minimization as described above, MD simulation was performed with a step size of 1 fs. The system was heated for 650 ps from 0 K to 300 K, in 5 K increment every 10 ps. After heating, equilibration run followed for 200 ps, during which velocities were rescaled if the temperature deviated from 300 K by more than 5 K. The final production run lasted 10 ns. Coordinates were recorded every 10 ps, totalling 1000 coordinate frames, with 56 triads per frame. To calculate stiffness, we made histograms of ω_{ni} ($n = 1 \cdots 56$, $i = 1, 2, 3$), with a bin size of 0.002 rad/Å (Fig. 2a,b). Fitting logarithm of this histogram with a quadratic curve (Fig. 2c,d) yields average and variance of ω_{ni}. We calculated stiffness by using Eq. 5.

Acknowledgments

We acknowledge helpful discussions with Mariappan Muthuchamy and Gerald Offer for providing the C code used in constructing straight leucine zipper coiled coils. This work was partially funded by the National Institute of Health (grant number: R21NS058604).

References

1. Adamovic I, Mijailovich S, Karplus M. The Elastic Properties of the Structurally Characterized Myosin II S2 Subdomain: A Molecular Dynamics and Normal Mode Analysis. Biophys J 2008;94(10):3779–3789. [PubMed: 18234833]
2. Arfken, G.; Weber, H. Academic Press. Vol. sixth. 1997. Mathematical Methods for Physics.
3. Brooks B, Bruccoleri R, Olafson B, States D, Swaminathan S, Karplus M. CHARMM: A program for macromolecular energy, minimization, and dynamics calculations. J Comp Chem 1983;4:187–217.
4. Brown J, Cohen C. Regulation of muscle contraction by tropomyosin and troponin: how structure illuminates function. Adv Protein Chem 2005;71:121–59. [PubMed: 16230111]
5. Brown J, Cohen C, Parry D. Heptad breaks in alpha-helical coiled coils: stutters and stammers. Proteins 1996;26(2):134–45. [PubMed: 8916221]
6. Brown J, Zhou Z, Reshetnikova L, Robinson H, Yammani R, Tobacman L, Cohen C. Structure of the mid-region of tropomyosin: Bending and binding sites for actin. Proc Natl Acad Sci USA 2005;102 (52):18,878–18,883.
7. Choe S, Sun SX. The elasticity of alpha-helices. J Chem Phys 2005;122(24):244912. [PubMed: 16035821]
8. Crick F. The packing of α-helices: simple coiled-coils. Acta Cryst 1953;6(89):689–697.
9. Gaffin R, Gokulan K, Sacchettini J, Hewett T, Klevitsky R, Robbins J, Muthuchamy M. Charged residue changes in the carboxy-terminus of α-tropomyosin alter mouse cardiac muscle contractility. J Physiol 2004;556(2):531–543. [PubMed: 14766940]
10. Goriely A, Tabor M. Nonlinear dynamics of filaments *i.* dynamical instabilities. Physica D 1997;105:20–44.
11. Greenberg M, Wang C, Lehman W, Moore J. Modulation of actin mechanics by caldesmon and tropomyosin. Cell Motil Cytoskeleton 2008;65(2):156–64. [PubMed: 18000881]

12. Humphrey W, Dalke A, Schulten K. VMD: Visual molecular dynamics. J Mol Graphics 1996;14(1): 33–38.
13. Hvidt S, Nestler FHM, Greaser ML, Ferry JD. Flexibility of myosin rod determined from dilute solution viscoelastic measurements. Biochemistry 1982;21:4064–4073. [PubMed: 7126531]
14. Lakkaraju S, Hwang W. Persistence Length vs. Critical Buckling Length:What governs a biofilament conformation? submitted. 2009
15. Landau, L.; Lifshitz, E. Theory of Elasticity. Vol. 7. Nauka, Moscow: 1987. Course of Theoretical Physics.
16. Lee D, Ivaninskii S, Burkhard P, Hodges R. Unique stabilizing interactions identified in the two-stranded alpha-helical coiled-coil: Crystal structure of a cortexillin I/gcn4 hybrid coiled-coil peptide. Protein Sci 2003;12:1395–1405. [PubMed: 12824486]
17. McLachlan A, Stewart M. The 14-fold periodicity in alpha-tropomyosin and the interaction with actin. J Mol Biol 1976;103(2):271–98. [PubMed: 950663]
18. Minakata S, Maeda K, Oda N, Wakabayashi K, Nitanai Y, Maeda Y. Two-Crystal Structures of Tropomyosin C-Terminal Fragment 176-273: Exposure of the Hydrophobic Core to the Solvent Destabilizes the Tropomyosin Molecule. Biophys J 2008;95(2):710–719. [PubMed: 18339732]
19. Naumanen P, Lappalainen P, Hotulainen P. Mechanisms of actin stress fibre assembly. J Microscopy 2008;231(3):446–454.
20. Neria E, Fischer S, Karplus M. Simulation of activation free energies in molecular systems. J Chem Phys 1996;105:1902–1921.
21. van Noort J, van der Heijden T, de Jager M, Wyman C, Kanaar R, Dekker C. The coiled-coil of the human Rad50 DNA repair protein contains specific segments of increased flexibility. Proc Natl Acad Sci USA 2003;100(13):7581–7586. [PubMed: 12805565]
22. Offer G, Sessions R. Computer modelling of the alpha-helical coiled coil:packing of side-chains in the inner core. J Mol Biol 1995;249:967–987. [PubMed: 7791220]
23. Olson TM, Kishimoto NY, Whitby FG, Michels VV. Mutations that alter the surface charge of alpha-tropomyosin are associated with dilated cardiomyopathy. J Mol Cell Cardiology 2001;33(4):723–732.
24. Park J, Kahng B, Kamm R, Hwang W. Atomistic Simulation Approach to a Continuum Description of Self-Assembled β-Sheet Filaments. Biophys J 2006;90(7):2510–2524. [PubMed: 16415051]
25. Perry S. Vertebrate tropomyosin: distribution, properties and function. J Mus Res Cell Motil 2001;22 (1):5–49.
26. Phillips G Jr, Chacko S. Mechanical Properties of tropomyosin and implications for muscle regulation. Biopolymers 1996;38:89–95. [PubMed: 8679944]
27. Phillips G Jr, Fillers J, Cohen C. Tropomyosin crystal structure and muscle regulation. J Mol Biol 1986;192(1):111–31. [PubMed: 3820299]
28. Reif, F. Fundamentals of Statistical and Thermal Physics. McGraw-Hill; Tokyo, Japan: 1965.
29. Schaefer M, Karplus M. A comprehensive analytical treatment of continuum electrostatics. J Phys Chem 1996;100:1578–1599.
30. Schaefer M, Bartels C, Leclerc F, Karplus M. Effective atom volumes for implicit solvent models: comparison between Voronoi volumes and minimum fluctuation volumes. J Comp Chem 2001;22:1857–1879. [PubMed: 12116417]
31. Singh A, Hitchcock-DeGregori SE. Tropomyosin's periods are quasi-equivalent for actin binding but have specific regulatory functions. Biochemistry 2007;46(51):14,917–14,927.
32. Whitby F, Phillips G Jr. Crystal Structure of Tropomyosin at 7 Angstroms Resolution. PROTEINS: Structure, Function, and Genetics 2000;38:49–59.
33. Wolgemuth C, Sun S. Elasticity of α-Helical Coiled Coils. Phys Rev Lett 2006;97(24):248,101–4.
34. Yu Y, Monera O, Hodges R, Privalov P. Ion Pairs Significantly Stabilize Coiled-coils in the Absence of Electrolyte. J Mol Biol 1996;255(3):367–372. [PubMed: 8568882]

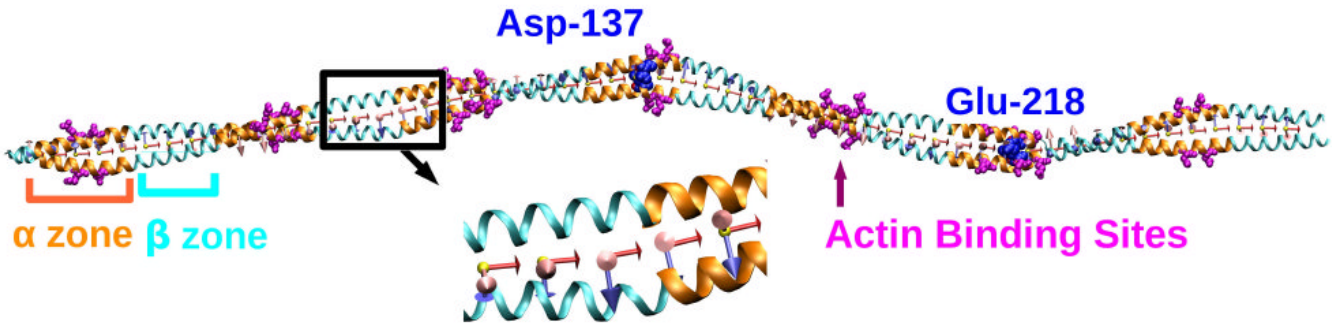

Fig. 1.

Crystal structure of a cardiac muscle tropomyosin (PDB ID: 1C1G).[32] The α and β zones are shown in orange and cyan, respectively. Successive α or β zones rotate by about 90° axially. Side chains of the putative actin binding residues[17] in α zones are shown in magenta. Asp137 and Glu218 are shown in blue van der Waals representation. Starting with triad 1 on the left (N-terminus), we assigned 56 triads along the length of the molecule in intervals of 5 residues. Triads 1 and 56 were not considered for the flexibility map to eliminate edge effects. The magnified image shows triads 14-18. $\mathbf{e}_3$ (red) points to the right, $\mathbf{e}_2$ (blue) points downward, and $\mathbf{e}_1$ (pink) points out of the page.

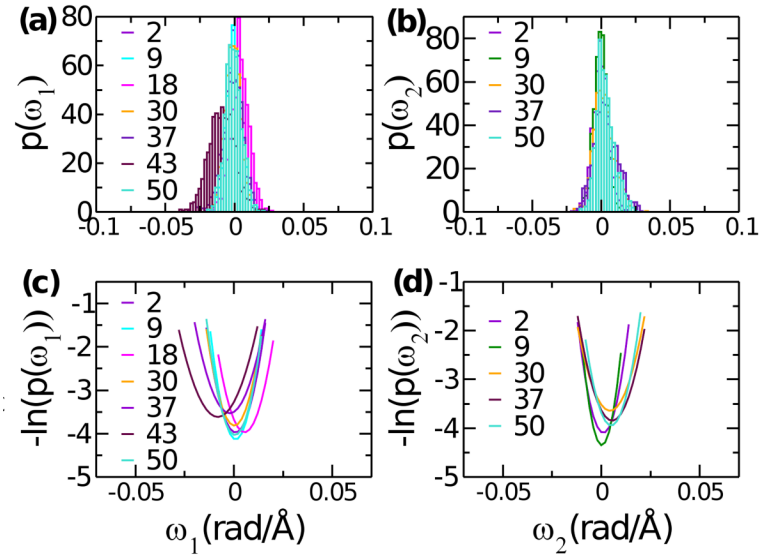

Fig. 2.

Example distributions of (a) ω_1 and (b) ω_2, and (c,d) quadratic fits to their logarithm. Corresponding triad numbers are marked in the graph. While equilibrium curvatures ω_{01} & ω_{02} are generally 0 along the length of tropomyosin, at triad 43 (lowest rigidity region Fig. 4 (b)) ω_{01} is about −0.01.

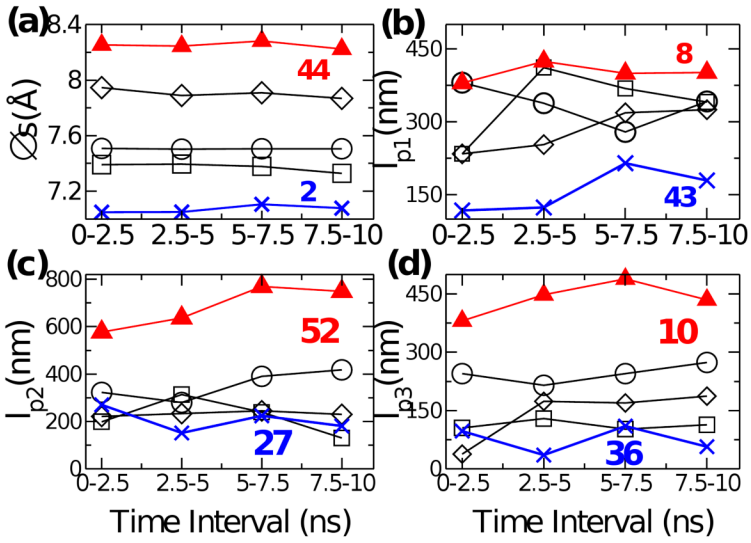

Fig. 3.

Time evolution of Δs and l_{pi} for select triads. Averages were made over 2.5-ns intervals, for triad 15 (circle), 30 (square) and 45 (diamond). Data for triads that occupy the minimum (blue cross) and maximum (red triangle) in Fig. 4 are also shown, with triad numbers marked.

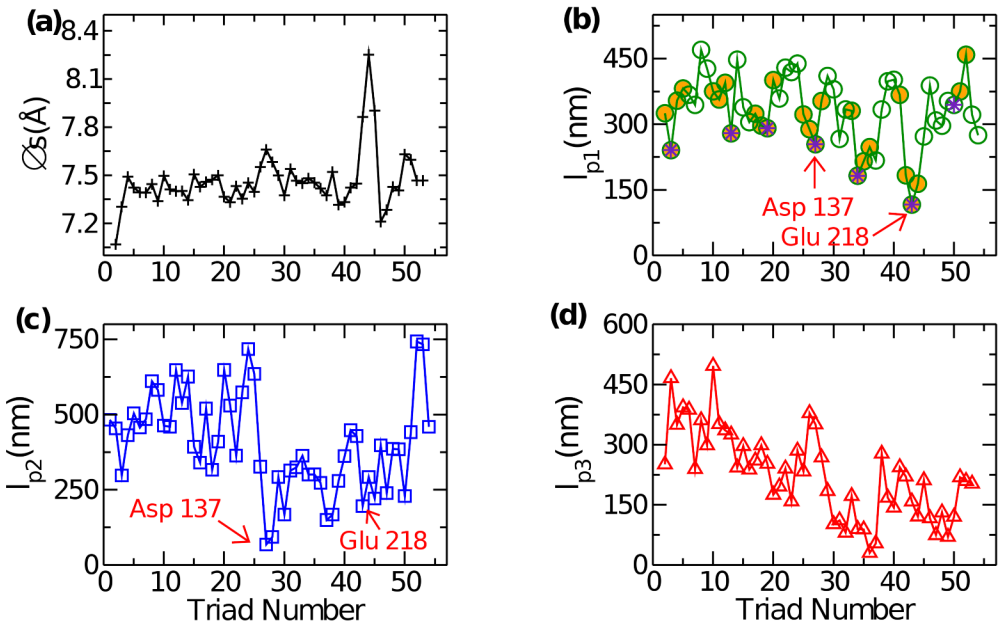

Fig. 4.

Flexibility map of Tropomyosin. (a) Δs, showing a jump near the most labile region at Glu218 (triad 43). (b) l_{p1} regarding local splay deformation. Minimum occurs again at triad 43. Marked in orange represent α zones (*cf.*, Fig. 1), which contain actin binding sites (magenta stars) that are locally the most flexible. (c) l_{p2} regarding bend of the broad face. (d) l_{p3} representing torsional stiffness. Overall, the molecule is more flexible towards the C-terminus.

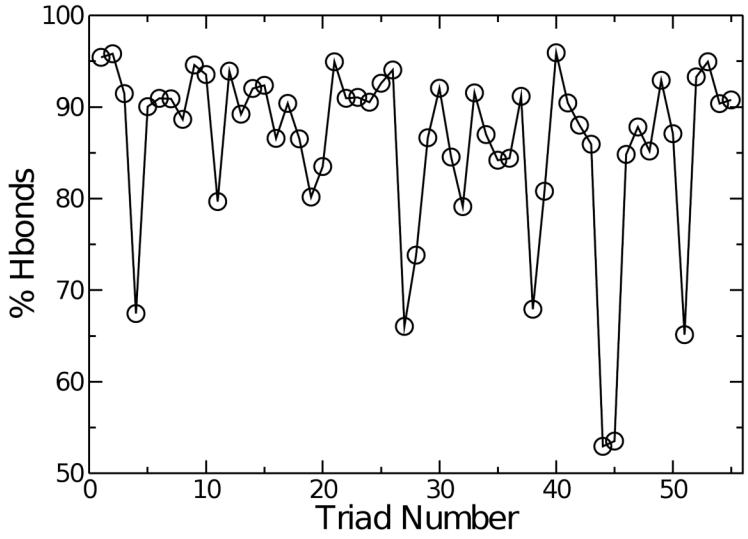

Fig. 5.

Occupancy of backbone hydrogen bonds during the simulation. A cutoff distance of 2.4 Å was used to identify hydrogen bond formation. Regions of low hydrogen bond occupancy correspond to labile regions in Fig. 4.

Table 1

Persistence length l_p of leucine zipper coiled-coil and mutants. Mutated residues are marked in bold. l_p drops with an increase in the number of point mutations along the hydrophobic core (*a* and *d* positions), while there is no significant effect by mutations in exposed residues. As reported previously,[14] in this range of coiled-coil sizes, there is a dependence of l_p on the length of the molecule, as can be seen by comparing wild-type (WT) values of 112- and 84-residue coiled-coils.

Size (no. of res)	No. of mutations	Residue No.	Sequence																											K_b ($\times 10^{-27}$ Nm^2)	l_p (nm)
			a	***b***	***c***	***d***	***e***	***f***	***g***	***a***	***b***	***c***	***d***	***e***	***f***	***g***	***a***	***b***	***c***	***d***	***e***	***f***	***g***	***a***	***b***	***c***	***d***	***e***	***f***	***g***	
112	WT	1	M	K	Q	L	E	D	K	V	E	E	L	L	S	K	N	Y	H	L	E	N	E	V	A	R	L	K	K	L	2.04	493.43
		29	M	K	Q	L	E	D	K	V	E	E	L	L	S	K	N	Y	H	L	E	N	E	V	A	R	L	K	K	L		
		57	M	K	Q	L	E	D	K	V	E	E	L	L	S	K	N	Y	H	L	E	N	E	V	A	R	L	K	K	L		
		85	M	K	Q	L	E	D	K	V	E	E	L	L	S	K	N	Y	H	L	E	N	E	V	A	R	L	K	K	L		
	10	1	M	K	Q	L	E	D	K	V	E	E	**K**	L	S	K	N	Y	H	**E**	E	N	E	V	A	R	L	K	K	L	1.52	362.30
		29	M	K	Q	**K**	E	D	K	V	E	E	**K**	L	S	K	N	Y	H	L	E	N	E	V	A	R	**E**	K	K	L		
		57	M	K	Q	**K**	E	D	K	V	E	E	L	L	S	K	N	Y	H	**E**	E	N	E	V	A	R	**K**	K	K	L		
		85	M	K	Q	L	E	D	K	V	E	E	**K**	L	S	K	N	Y	H	**E**	E	N	E	V	A	R	L	K	K	L		
	14	1	M	K	Q	L	E	D	K	V	E	E	**K**	L	S	K	N	Y	H	**E**	E	N	E	V	A	R	**E**	K	K	L	1.21	287.41
		29	M	K	Q	**K**	E	D	K	V	E	E	**K**	L	S	K	N	Y	H	**E**	E	N	E	V	A	R	**E**	K	K	L		
		57	M	K	Q	**K**	E	D	K	V	E	E	**K**	L	S	K	N	Y	H	**E**	E	N	E	V	A	R	**K**	K	K	L		
		85	M	K	Q	**K**	E	D	K	V	E	E	**K**	L	S	K	N	Y	H	**E**	E	N	E	V	A	R	L	K	K	L		
	16	1	M	K	Q	**K**	E	D	K	V	E	E	**K**	L	S	K	N	Y	H	**E**	E	N	E	V	A	R	**E**	K	K	L	0.82	198.07
		29	M	K	Q	**K**	E	D	K	V	E	E	**K**	L	S	K	N	Y	H	**E**	E	N	E	V	A	R	**E**	K	K	L		
		57	M	K	Q	**K**	E	D	K	V	E	E	**K**	L	S	K	N	Y	H	**E**	E	N	E	V	A	R	**K**	K	K	L		
		85	M	K	Q	**K**	E	D	K	V	E	E	**K**	L	S	K	N	Y	H	**E**	E	N	E	V	A	R	**E**	K	K	L		
84	WT	1	M	K	Q	L	E	D	K	V	E	E	L	L	S	K	N	Y	H	L	E	N	E	V	A	R	L	K	K	L	1.41	343.01
		29	M	K	Q	L	E	D	K	V	E	E	L	L	S	K	N	Y	H	L	E	N	E	V	A	R	L	K	K	L		
		57	M	K	Q	L	E	D	K	V	E	E	L	L	S	K	N	Y	H	L	E	N	E	V	A	R	L	K	K	L		
	30	1	M	**L**	Q	L	**L**	D	**L**	V	**L**	**L**	L	L	S	**L**	N	Y	H	L	**L**	N	**L**	V	A	**L**	L	**L**	K	L	1.42	338.20
		29	M	**L**	Q	L	**L**	D	**L**	V	**L**	**L**	L	L	S	**L**	N	Y	H	L	**L**	N	**L**	V	A	**L**	L	**L**	K	L		
		57	M	**L**	Q	L	**L**	D	**L**	V	**L**	**L**	L	L	S	**L**	N	Y	H	L	**L**	N	**L**	V	A	**L**	L	**L**	K	L		